Eur. Phys. J. A **16**, 171–175 (2003)
DOI 10.1140/epja/i2002-10092-x

THE EUROPEAN
PHYSICAL JOURNAL A

# Maximally aligned states in $^{99}$Ag

D. Sohler[1,a], Zs. Dombrádi[1], J. Blomqvist[2], J. Cederkäll[2,3], J. Huijnen[4], M. Lipoglavšek[5], M. Palacz[6], A. Ataç[7], C. Fahlander[8], H. Grawe[9], A. Johnson[2], A. Kerek[2], W. Klamra[2], J. Kownacki[6], A. Likar[5], L.-O. Norlin[2], J. Nyberg[7], J. Persson[7], D. Seweryniak[10], G. de Angelis[11], P. Bednarczyk[11,12,13], D. Foltescu[14], D. Jerrestam[15], S. Juutinen[16], E. Mäkelä[16], M. de Poli[11], H.A. Roth[14], T. Shizuma[17], Ö. Skeppstedt[14], G. Sletten[17], J. Timár[1], S. Törmänen[17], and M. Weiszflog[18]

1 Institute of Nuclear Research, Debrecen, Hungary
2 Department of Physics, Royal Institute of Technology, Stockholm, Sweden
3 CERN, Geneva, Switzerland
4 The Svedberg Laboratory, Uppsala University, Uppsala, Sweden
5 J. Stefan Institute, Ljubljana, Slovenia
6 Heavy Ion Laboratory, University of Warsaw, Warsaw, Poland
7 Department of Radiation Sciences, Uppsala University, Uppsala, Sweden
8 Department of Physics, Lund University, Lund, Sweden
9 GSI, Darmstadt, Germany
10 Argonne National Laboratory, Chicago, USA
11 Laboratori Nazionali di Legnaro, Padova, Italy
12 Institute de Recherches Subatomiques, Strasbourg, France
13 The Niewodniczanski Institute of Nuclear Physics, Krakow, Poland
14 Chalmers University of Technology, Gothenburg, Sweden
15 Department of Neutron Research, Uppsala University, Nyköping, Sweden
16 Department of Physics, University of Jyväskylä, Jyväskylä, Finland
17 Niels Bohr Institute, University of Copenhagen, Copenhagen, Denmark
18 Department of Neutron Research, Uppsala University, Uppsala, Sweden

Received: 18 June 2002 / Revised version: 2 September 2002 /
Published online: 4 February 2003 – 
Communicated by J. Äystö

**Abstract.** Excited states of $^{99}$Ag were populated via the $^{50}$Cr + $^{58}$Ni (261 MeV) reaction using the NORDBALL detector array equipped with charged-particle and neutron detector systems for reaction channel separation. On the basis of the measured $\gamma\gamma$-coincidence relations and angular distribution ratios a significantly extended level scheme has been constructed up to $E_x \sim 7.8$ MeV and $I = 35/2$. The experimental results were described within the framework of the shell model. Candidates for states fully aligned in the $\pi g_{9/2}^{-3} \nu(d_{5/2}, g_{7/2})^2$ valence configuration space were found at 4109 and 6265 keV.

**PACS.** 21.10.Hw Spin, parity, and isobaric spin – 23.20.Lv Gamma transitions and level energies – 21.60.Cs Shell model – 27.60.+j 90 ≤ A ≤149

## 1 Introduction

It is always a challenge to go beyond the standard shell model description of a nucleus. This can be achieved by exciting it to a high spin value which falls out of the conventional valence space. Such an attempt can be realized in the easiest way close to the doubly magic nuclei. In our experiment [1] devoted to study nuclei in the vicinity of $^{100}$Sn, the maximally spin aligned states have been reached in $^{98}$Ag [2], as well as in $^{98}$Pd [3]. In this experiment a substantial amount of new experimental data on $^{99}$Ag was also collected, making it possible to go beyond the valence shell excitations in this case, too.

The low-lying levels of $^{99}$Ag have already been investigated from $\beta$-decay studies [4,5]. Some of the higher spin states were excited via the $^{64}$Zn($^{40}$Ca, 3p2n) heavy-ion reaction [6]. These measurements led to a fairly well-established level scheme up to 2.6 MeV and the yrast states have been observed up to the 3929 keV $(27/2^+)$ level.

[a] e-mail: sohler@atomki.hu

The aim of the present work was to extend the available information on excited levels of $^{99}$Ag up to the energy region where the maximally aligned and core excited states are expected to appear in the level scheme.

## 2 Experimental methods

The experiment was carried out at the Tandem accelerator Laboratory of the Niels Bohr Institute using the NORDBALL multidetector array [7,8]. Two $^{50}$Cr targets enriched to 96.8% were used with thicknesses of 4.8 and 3.1 mg/cm$^2$ deposited on gold backings of 11 and 19.5 mg/cm$^2$, respectively. The $^{50}$Cr targets were bombarded with a 261 MeV beam of $^{58}$Ni. The setup consisted of 15 BGO-shielded Ge detectors and 30 $BaF_2$ crystals covering the backward $2\pi$ hemisphere. The Ge detectors were placed in three rings at angles of 79.1°, 100.9° and 142.6° with respect to the beam direction. Their total photo-peak efficiency was $\sim$ 1% at 1.3 MeV. The $BaF_2$ calorimeter provided information on the total $\gamma$-ray multiplicity and sum energy. Furthermore, the logical OR signal from the $BaF_2$ detectors gave the time reference for all other signals. For reaction channel identification the $\gamma$-rays were measured in coincidence with the charged particles and the neutrons emitted by the $^{108}$Te compound nucleus. The detection of light charged particles was performed by means of a 21-element $\Delta E$-type silicon ball covering about 90% of the total solid angle [9]. The difference in stopping powers of protons and $\alpha$-particles was used to discriminate between them. The average efficiency for the detection and identification of protons and $\alpha$-particles was about 60% and 40%, respectively. The forward $1\pi$ solid angle was covered by the Neutron Wall consisting of 11 liquid scintillator detectors assisting in deducing the neutron multiplicity of each event [10]. The neutron and $\gamma$-ray signals in the neutron detectors were distinguished by a pulse shape discrimination technique based on the zero–cross-over principle combined with a time-of-flight method [11,12]. The neutron detection efficiency was about 24%.

An event was recorded on magnetic tape if at least two $\gamma$-rays were detected in the Ge detectors with a maximum time difference of 80 ns and at least one $\gamma$-ray in the $BaF_2$ calorimeter, or at least one Ge detector and one $BaF_2$ crystal fired in coincidence with at least one neutron detected in the liquid scintillators. Ge signals delayed by a maximum of $\sim$ 900 ns were read out if a trigger condition was fulfilled. A total of about $2.5 \times 10^9$ events were collected and then sorted into a set of $\gamma\gamma$-coincidence matrices by requiring different conditions on the number of detected charged particles and neutrons.

The $^{99}$Ag nucleus was populated with the emission of one proton and two $\alpha$-particles from the compound nucleus. The relative yield for this reaction channel was about 0.4%. The $1p2\alpha$-particle–gated $\gamma\gamma$-coincidence matrix contained also the $\gamma$-rays of $^{98}$Pd and $^{98}$Ag since some of the emitted particles were not detected. Subsequent $\gamma$ gating resolved these leakages. In order to improve the statistics the $2\alpha$-gated $\gamma\gamma$-coincidence matrix was added to the $1p2\alpha$-gated one. This introduced the contamination from $^{100}$Cd, which, however, caused only a minor problem due to the very weak population of $^{100}$Cd via this reaction channel. The $\gamma\gamma$-coincidence matrices were analyzed in detail using a standard gating procedure with the help of the RADWARE software package [13]. The sum of the spectra gated with the 335, 686, 804, 894, 916 and 1221 keV transitions is shown in fig. 1 where the $\gamma$-rays assigned to $^{99}$Ag are labelled. Typical $\gamma\gamma$-coincidence spectra are presented in fig. 2.

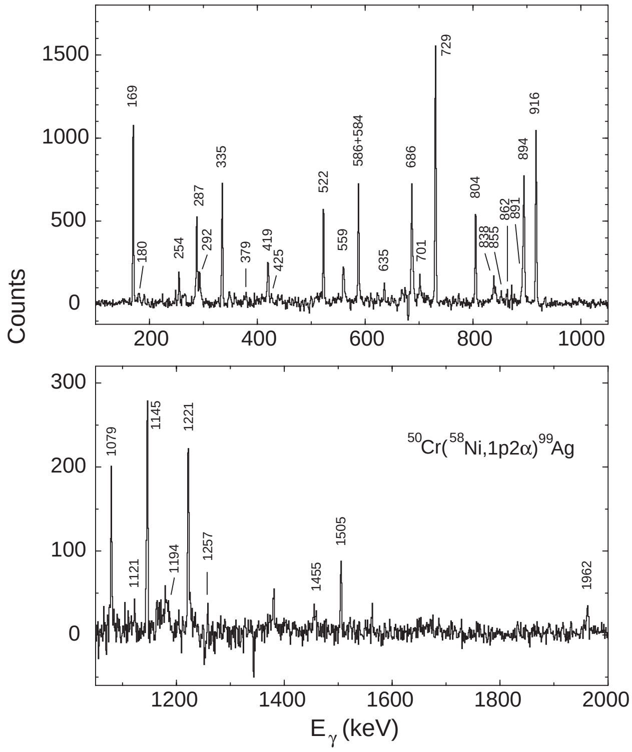


**Fig. 1.** The sum of the spectra gated with the 335, 686, 804, 894, 916 and 1221 keV $\gamma$-rays in the sum of the $\gamma\gamma$-coincidence matrices gated by 1 proton, 2 $\alpha$-particles and 0 proton, 2 $\alpha$-particles.

The multipolarities of the $\gamma$-rays were obtained by means of a simplified $\gamma\gamma$-correlation analysis. The angular distribution ratio

$$R_{\text{ang}} = \frac{I_\gamma(143^\circ)}{I_\gamma(79^\circ) + I_\gamma(101^\circ)}$$

deduced from the intensity of a transition detected at 143° and at 79° or at the equivalent 101° angle relative to the beam direction in coincidence with a $\gamma$-ray observed at any direction, is sensitive to the angular momentum transferred by the $\gamma$-ray. In order to reduce the uncertainty of the measured $R_{\text{ang}}$ values, we took the weighted average of several intensity ratios determined by using different coincident $\gamma$-rays as gating transitions. The dependence of $R_{\text{ang}}$ ratios on the multipolarity of the gating transition was found normally to be smaller than the typical uncertainties in the peak fitting [14]. Because of this neglected effect $\Delta R_{\text{ang}} = 0.1$ systematic error was taken into account in the uncertainties given in table 1. According

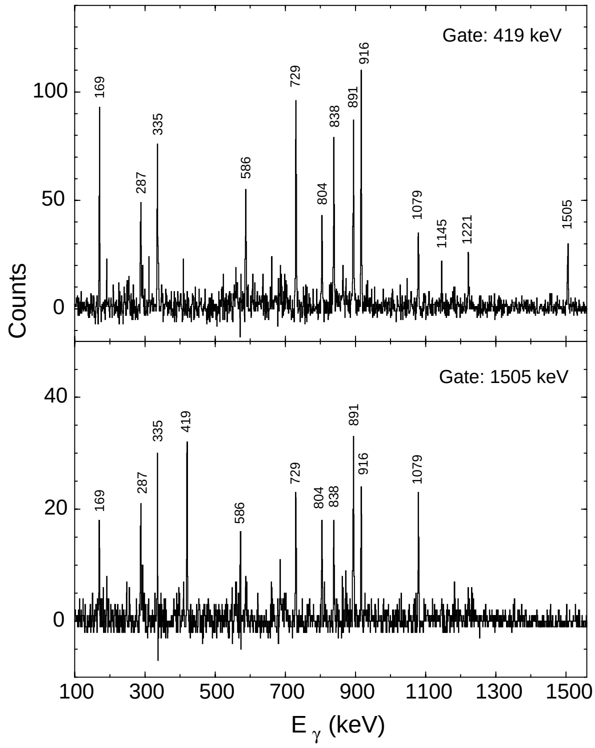


**Fig. 2.** Typical $\gamma\gamma$-coincidence spectra of $^{99}$Ag obtained from the sum of the matrices gated by 1 proton, 2 $\alpha$-particles and 0 proton, 2 $\alpha$-particles.

to theoretical estimations on the NORDBALL geometry, $R_{\text{ang}} \sim 1.5$ corresponds to a stretched quadrupole or a non-stretched dipole transition, and $R_{\text{ang}} \sim 0.8$ to a stretched dipole one [15]. For mixed transitions $R_{\text{ang}}$ ratios can be distributed between 0.3 and 1.8 depending on the spin difference between the initial and final states and on the $\delta$ mixing ratio of the $\gamma$-ray [15]. This kind of ambiguity could only be resolved by performing a full angular correlation analysis on a higher statistics data set. During the multipolarity assignments only dipole and electric quadrupole transitions were considered. In addition, it was assumed that in the heavy-ion induced fusion-evaporation reaction high spin states are preferably populated and the decays mainly proceed via stretched transitions along the yrast line. Thus, the maximum possible spin value allowed by the angular distribution ratios and by the coincidence relationships of the transitions was assigned to the states. Definite parity could be assigned to a state if $E2$ multipolarity was determined for one of its de-exciting transitions.

## 3 Results

Table 1 contains the energies, relative intensities and angular distribution ratios of the $\gamma$ transitions in $^{99}$Ag together with the deduced spins for their initial and final states. The energies and intensities of the $\gamma$-rays were determined from the $\gamma\gamma$-coincidence matrices. The systematic errors due to the energy and efficiency calibrations were estimated to be $\sim 0.3$ keV and $\sim 5\%$, respectively. A total of 33 transitions were assigned to the studied nucleus, 21 of which are new. The assignment of the 600.5 keV $\gamma$-ray to $^{99}$Ag [6] could not be confirmed by our coincidence measurement.

**Table 1.** Energies, relative intensities and angular distribution ratios of transitions together with the deduced spins of the initial and final states from the $^{50}$Cr($^{58}$Ni, 1p2$\alpha$)$^{99}$Ag reaction.

| $E_\gamma$ (keV) | $I_\gamma$ (rel.) | $R_{\text{ang}}$ | $E_i$ (keV) | $I_i^\pi \to I_f^\pi$ |
|---|---|---|---|---|
| 168.7(3) | 33.6(23) | 0.83(12) | 3929 | $27/2^+ \to 25/2^+$ |
| 180.1(4) | 3.4(4) | | 4109 | $\to 27/2^+$ |
| 254.1(3) | 3.3(4) | 0.61(20) | 3125 | $23/2^+ \to 21/2^+$ |
| 287.2(4) | 7.8(12) | 0.77(15) | | |
| 292.4(4) | 2.3(3) | | | |
| 334.6(3) | 29.9(42) | 0.86(12) | 1980 | $19/2^+ \to 17/2^+$ |
| 379.2(4) | 2.1(4) | | 3929 | $27/2^+ \to$ |
| 419.1(3) | 10.1(8) | 0.82(14) | 6265 | $33/2 \to 31/2$ |
| 424.6(4) | 4.6(7) | | 3550 | $\to 23/2^+$ |
| 522.3(3) | 19.7(21) | 0.72(14) | 5137 | $31/2 \to 29/2^+$ |
| 559.1(3) | 9.1(19) | 0.82(17) | 2539 | $21/2^+ \to 19/2^+$ |
| 584.0(6) | 2.1(3) | | 6475 | $\to 29/2$ |
| 586.3(3) | 36.5(26) | 0.81(12) | 3125 | $23/2^+ \to 21/2^+$ |
| 635.4(3) | 8.1(8) | | 3760 | $25/2^+ \to 23/2^+$ |
| 685.8(3) | 45.2(34) | 0.73(12) | 4615 | $29/2^+ \to 27/2^+$ |
| 701.0(4) | 3.7(6) | | 5838 | $\to 31/2$ |
| 729.4(3) | 98.0(77) | 1.50(14) | 1645 | $17/2^+ \to 13/2^+$ |
| 804.1(3) | 41.2(29) | 1.38(14) | 3929 | $27/2^+ \to 23/2^+$ |
| 837.8(3) | 13.3(11) | 0.86(20) | 5846 | $31/2 \to 29/2$ |
| 854.6(4) | 4.0(6) | | 4615 | $29/2^+ \to 25/2^+$ |
| 862.4(4) | 8.0(8) | | 3733 | $\to 21/2^+$ |
| 891.4(3) | 10.6(22) | | 2871 | $21/2^+ \to 19/2^+$ |
| 893.8(3) | 72.2(64) | 1.47(17) | 2539 | $21/2^+ \to 17/2^+$ |
| 916.0(3) | 100.0(81) | 1.56(18) | 916 | $13/2^+ \to 9/2^+$ |
| 1079.0(5) | 16.0(18) | 0.69(18) | 5008 | $29/2 \to 27/2^+$ |
| 1121.4(6) | 2.1(4) | | 7596 | |
| 1145.4(3) | 17.1(24) | 1.38(21) | 3125 | $23/2^+ \to 19/2^+$ |
| 1194.1(4) | 5.3(7) | | 3733 | $\to 21/2^+$ |
| 1221.4(3) | 28.1(24) | 1.42(18) | 3760 | $25/2^+ \to 21/2^+$ |
| 1257.0(5) | 4.2(6) | | 6265 | $33/2 \to 29/2$ |
| 1454.8(3) | 2.7(6) | | 7293 | |
| 1504.8(3) | 5.0(6) | 0.66(15) | 7770 | $35/2 \to 33/2$ |
| 1961.7(5) | 5.1(8) | 0.74(30) | 5891 | $29/2 \to 27/2^+$ |

In the course of angular distribution analysis stretched dipole or stretched quadrupole multipolarity was assigned to a $\gamma$-ray if its $R_{\text{ang}}$ value was equal to the corresponding theoretical values 0.8 or 1.5 within $1\sigma$ uncertainty ($< 20\%$). Although, the 254, 1079 and 1962 keV transitions decaying from the 3125, 5008, 5891 keV levels have angular distribution ratios with too high uncertainty ($> 20\%$), we could exclude the $\varDelta I = 2$ stretched quadrupole possibility since their $R_{\text{ang}}$ values were less than 0.8 (see table 1). The obtained $R_{\text{ang}}$ values are in agreement with the angular distribution results given by Piel *et al.* [6] for the transitions observed also by them.

The proposed level scheme shown in fig. 3 was constructed on the basis of $\gamma\gamma$-coincidence relations, energy and intensity balances. The order of the transitions in the

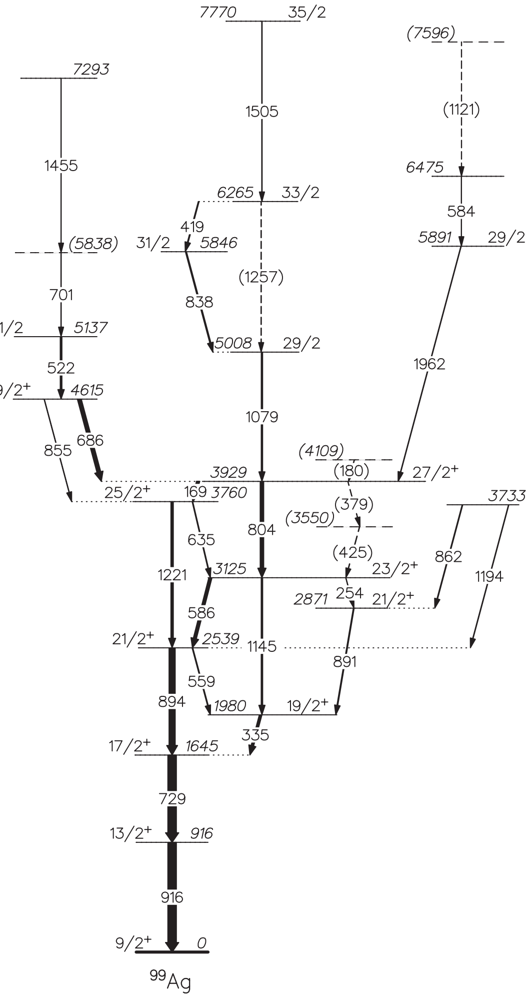


**Fig. 3.** Proposed level schemes of $^{99}$Ag populated in the reaction $^{50}$Cr($^{58}$Ni, p2$\alpha$).

$\gamma$-ray cascades was deduced from the intensity relations. This level scheme is basically consistent with the previous results [6] except for some minor differences. The 686 keV transition was placed at higher excitation energy. Also the 287 keV $\gamma$-ray should be located at higher excitation energy than it was put previously [6]. However, we could not firmly place this transition in the level scheme. The existence of the state at 3760 keV is now supported also by the coincidence relations of the new 635 keV linking transition. The 3929 and 1980 keV states are connected, beside the 169-635-586-559 keV and the 804-1145 keV branches, also via another cascade establishing the 2871 and the 3550 keV levels. The latter one remains ambiguous due to the uncertain order of the 379 and 425 keV transitions. This cascade is probably continued by a 180 keV $\gamma$-ray depopulating the tentative level at 4109 keV. An additional side feeding of the states at 2539 and 2871 keV comes from the level at 3733 keV. Above the 3929 keV state the level scheme is split up into three separate branches. One of them is started at 7293 keV and includes other new levels at 4615, 5137 and 5838 keV. Another $\gamma$-ray sequence feeds the low-lying part of the level scheme by connecting the new states at 7770, 6265, 5846 and 5008 keV to it. A third parallel cascade, feeding the 3929 keV state, is formed by the higher-energy 1962, the weak 584 and the tentative 1121 keV transitions establishing the levels at 5891, 6475 and 7596 keV.

The $9/2^+$ spin and parity assumption for the ground state is in agreement with the characteristics of the $\beta$-decay of $^{99}$Ag [4]. The previously deduced spin-parity values of $13/2^+$, $17/2^+$, $19/2^+$, $21/2^+$, $(23/2^+)$ and $(27/2^+)$ to the 916, 1645, 1980, 2539, 3125 and 3929 keV excited states, respectively, [6] are strengthened by our angular distribution ratios. Unambiguous spin-parity values could be deduced for all the above states, therefore, we have shown these values without parenthesis in fig. 3.

A stretched dipole character was deduced for the 254 keV $\gamma$-ray from its angular distribution ratio, thus, a $I^\pi = 21/2^+$ spin-parity value is proposed for the state at 2871 keV. On the basis of the $R_{\rm ang}$ ratio of the 1221 keV transition, $I^\pi = 25/2^+$ was assigned to the 3760 keV state.

One of the parallel branches is connected to the $I^\pi = 27/2^+$ state at 3929 keV by the strong 686 keV dipole transition and to the $I^\pi = 25/2^+$ state at 3760 keV by the weaker 855 keV $\gamma$-ray. Thus, we assign a $29/2^+$ spin-parity value to the 4615 keV level according to the above criteria. As a stretched dipole character was determined for the 522 keV $\gamma$-ray populating the 4615 keV state, a $I = 31/2$ spin value is assigned to the level at 5137 keV. In the second sequence spins can be assigned up to $I = 35/2$ corresponding to the obtained angular distribution ratios. Since a stretched dipole character was deduced for the 1079 keV transition feeding the $27/2^+$ state at 3929 keV, we could not deduce the parity for this sequence. The third cascade, feeding the 3929 keV state, decays to the lower-lying part via a higher-energy dipole transition. Thus, a $I = 29/2$ spin is assigned to the state at 5891 keV.

## 4 Discussion

The excited states in $^{99}$Ag can be interpreted in terms of the shell model. The states can be described by angular-momentum coupling of three $g_{9/2}$ proton holes with two neutrons in the $g_{7/2}, d_{5/2}, d_{3/2}, s_{1/2}$, and $h_{11/2}$ orbits.

Energies of the states of $^{99}$Ag were calculated by diagonalization in the full 6-shell basis. The matrix elements of the effective interaction are given in ref. [16]. The calculated and measured energies are compared in fig. 4. As can be seen, the energies of the experimental states are described with a reasonable precision. The differences between the experimental and calculated energies are less than 200 keV. From the three proton holes on the $g_{9/2}$ orbit, states up to spin 21/2 can be constructed. Combining them with two $d_{5/2}$ neutrons the maximum spin value is 29/2, while putting a neutron into the $g_{7/2}$ orbit the fully aligned state will be obtained at spin 33/2. According to the shell model calculations the yrast states up to spin $29/2^+$ are expected to arise mainly from the $\pi g^3_{9/2} \nu d^2_{5/2}$ configuration, while the second states in this spin region,

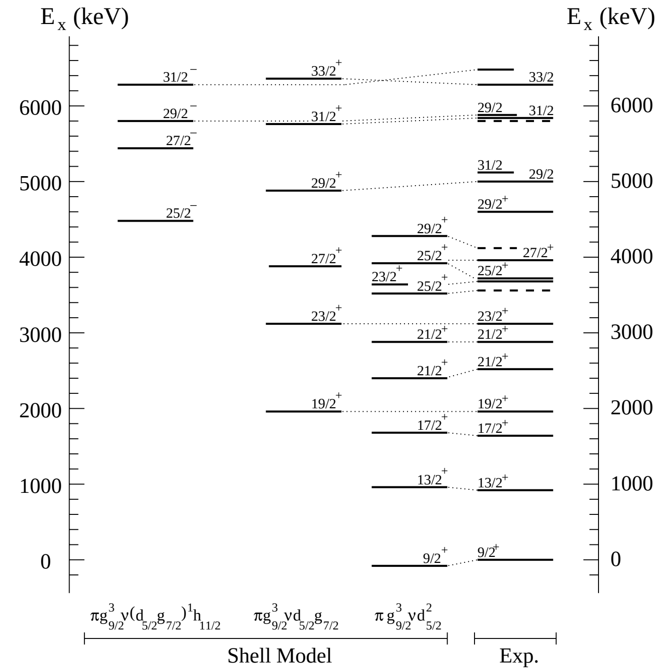


**Fig. 4.** Experimental levels of $^{99}$Ag are compared with the theoretical states calculated in the framework of the shell model. The horizontal dashed lines show tentative experimental levels.

as well as the yrast states up to $33/2^+$ come from the $\pi g^3_{9/2}\nu d_{5/2}g_{7/2}$ configuration. All the yrast states up to $33/2^+$ have been found experimentally, in addition some of the yrare states in the 21/2–$29/2^+$ spin region were identified. The 4109 keV state is a candidate for the fully aligned $\pi g^3_{9/2}\nu d^2_{5/2}$ state, while the 6265 keV state was assigned to the fully aligned $\pi g^3_{9/2}\nu d^1_{5/2}g^1_{7/2}$ configuration.

According to the calculations the two states at 5891 and 6475 keV may arise from a configuration obtained by exciting a neutron to the $h_{11/2}$ orbit.

It can be seen in fig. 4 that, in addition to the set of states assigned to shell model configurations, there remains a small group of states which do not have theoretical counterparts. These states may arise from excitations which originate from outside the model space used in the present work.

This work was supported by the Danish, Finnish and Swedish Natural Science Research Councils, The Hungarian Fund for Scientific Research (OTKA Contract No. D34587,T30497), and Polish Scientific Research Committee, grant no. 5P03B 046 20.

## References

1. H. Grawe *et al.*, Z. Phys. A **358**, 185 (1997).
2. J. Cederkäll *et al.*, Eur. Phys. J. A **1**, 7 (1998).
3. J. Cederkäll *et al.*, Z. Phys. A **359**, 227 (1997).
4. M. Huyse, Nucl. Phys. A **352**, 247 (1981).
5. A.W.B. Kalshoven, Nucl. Phys. A **337**, 120 (1980).
6. W.F. Piel *et al.*, Phys. Rev. C **37**, 1067 (1988).
7. B. Herskind, Nucl. Phys. A **447**, 395c (1985).
8. G. Sletten *Proceedings of the International Seminar on the Frontier of Nuclear Spectroscopy, Kyoto, Japan, 1992* (World Scientific, Singapore, 1993).
9. T. Kuroyanagi *et al.*, Nucl. Instrum. Methods A **316**, 289 (1992).
10. S.E. Arnell *et al.*, Nucl. Instrum. Methods A **300**, 303 (1991).
11. D. Wolski *et al.*, Nucl. Instrum. Methods A **360**, 584 (1995).
12. A. Johnson *et al.*, Nucl. Phys. A **557**, 401c (1993).
13. D. Radford, Nucl. Instrum. Methods A **361**, 297; 306 (1995).
14. S. Törmänen, PhD Thesis, University of Jyväskylä (1996).
15. M. Palacz, PhD Thesis, Soltan Institute for Nuclear Studies, Swierk, Poland (1996); M. Palacz *et al.*, Nucl. Phys. A **627**, 162 (1997).
16. D. Sohler *et al.*, Nucl. Phys. A **708**, 181 (2002).